JOURNAL OF MATERIALS SCIENCE 24 (1989) 4253–4260

Intermediate temperature oxidation in silicon nitride yttria ceramics

KAMAL E. AMIN, KERRY N. SIEBEIN, JONATHAN A. WADE
Norton Company, Advanced Ceramics, Northboro, Massachusetts 01532, USA

Silicon nitride billets with both 4% and 8% Y_2O_3 additives have been subjected to oxidation treatments for up to 300 h, in air, in the temperature range 700 to 1000° C. Flexure strength and weight gain measurements together with both scanning and transmission electron microscopy and X-ray diffraction studies were conducted on these billets in an effort to understand the oxidation process. It appears that the degradation phenomena is associated with both the formation of phases outside the Si_3N_4–Si_2ON_2–$Y_2Si_2O_7$ compatibility triangle of the system Si_3N_4–SiO_2–Y_2O_3 and with the decomposition of W-containing phases at and near the grain boundaries.

1. Introduction

Oxidation of Si_3N_4 has been shown to occur in the presence of both high and low oxygen partial pressure. At high oxygen partial pressures and temperatures over 1000° C, a dense oxide layer forms sealing off all surface pores. Weight gained during this process follows a parabolic law as a function of time [1]. While at low oxygen partial pressures, $< 8 \times 10^{-4}$ atm, an active oxidation process characterized by weight loss due to the formation of gaseous SiO_2 takes place [2]. Lange *et al.* [3] discovered that Si_3N_4 compositions containing high concentrations of Y_2O_3, 8% and higher, suffer severe property degradation when exposed to air for long periods of time at intermediate temperatures, < 1000° C. They attributed this phenomenon to the large change in molar volume associated with the formation of phases, and their oxidation products, which are outside the so-called compatibility triangle Si_3N_4–Si_2ON_2–$Y_2Si_2O_7$ of the system Si_3N_4–SiO_2–Y_2O_3. Gazza [4], however, indicated that phase instabilities and resultant crack formation were not always found in oxidized Si_3N_4 containing quaternary oxynitrides. Mangles and Bar [5] showed that for optimum intermediate temperature oxidation resistance in the range 700 to 1000° C, the presence of only one single phase at the grain boundaries of Si_3N_4, namely $Y_2Si_2O_7$, is essential. Their patent clearly demonstrates that both the temperature and nitrogen gas pressure of the final sintering cycles of RBSN (with Y_2O_3 additives), as well as the encapsulating powder mixtures of BN, Si_3N_4, SiO_2 and Y_2O_3, are critical to the process of achieving a thermally stable, single phase or phases at the grain boundaries. Apparently higher SiO_2 content of the encapsulating powder mixture, 15% to 25% by weight, helps the formation of $Y_2Si_2O_7$ single phase thus resulting in better oxidation resistance. However, according to Arias [6] at NASA, the presence of SiO_2 at levels higher than 11% by weight decreases the high-temperature strength of the sintered material. Work by Weaver and Lucek [7] at Norton shows that Si_3N_4 disintegrates after intermediate temperature oxidation for yttria content 8% and higher. Lucek [8] showed that those Si_3N_4 billets with 8% Y_2O_3 do not show loss of strength after exposure at 900 and 1000° C. Govila *et al.* [9] found that an Si_3N_4 + 8% Y_2O_3, which suffers accelerated weight gain at 1000° C, but only around 10% degradation in room-temperature strength after static oxidation for 300 h at 1000° C, nevertheless shows extreme sensitivity to early failure during stress rupture testing at 1000° C. At 1000° C and an applied stress of 138 MPa, failure times of the order of 50 h were observed. At 1200° C, and a stress of 344 MPa, no failures were observed after 260 h.

The literature shows a lack of agreement on the desirable Si_3N_4 compositions needed to achieve good oxidation resistance; some researchers recommend limiting the Al_2O_3 content to < 2% (Quackenbush [10] at GTE and Arias [6]), and SiO_2 to < 11.2% and C to < 0.2% (Gazza [4] at AMMRC and Schoun [11] at NASA).

The present investigation was conducted to determine the effect of yttria content on the intermediate temperature oxidation phenomena for Si_3N_4 compositions within the compatibility triangle (Si_3N_4–Si_2ON_2–$Y_2Si_2O_7$) and to characterize the resulting microstructure in an effort to determine factors contributing to the degradation process.

2. Experimental procedure

Silicon nitride billets containing both 4% and 8% Y_2O_3 were prepared by hot pressing. Standard Norton MOR bars, 0.125 in × 0.128 in × 2 in. (~0.32 cm × 0.325 cm × 5.08 cm) were machined from these billets for room-temperature four-point bend tests. The bend strength was measured using 1 in (2.54 cm) span quarter-point loading on samples in both the as-received and oxidized condition. Oxidation treatments were conducted in still air, in a resistance furnace. The test bars were placed on high-purity

0022–2461/89 $03.00 + .12

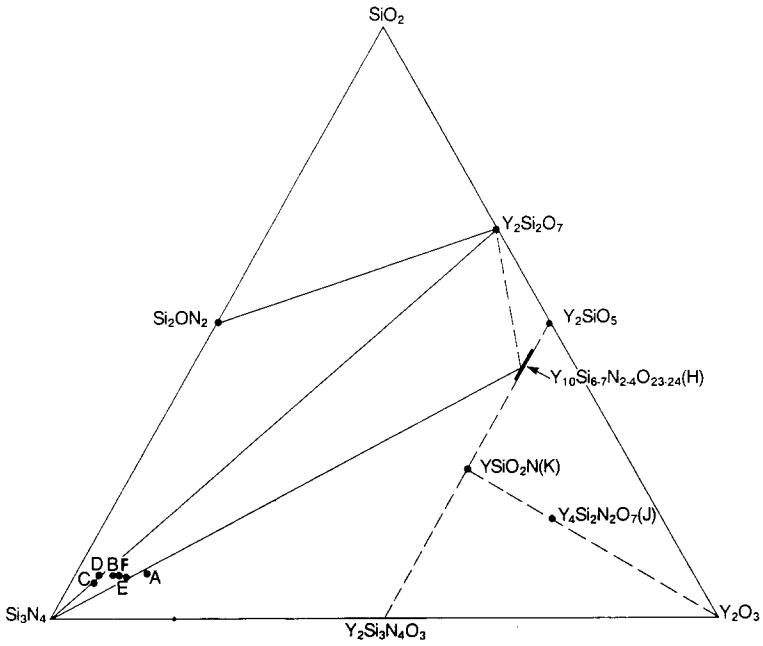

Figure 1 Ternary-phase diagram of the system Si_3N_4–Y_2O_3–SiO_2 showing the location of investigated compositions of billets A to F. Billet compositions are given in Table I.

Al_2O_3 knife edges for the 700 to 1000° C exposures. Weight changes were determined using a Mettler microbalance with sensitivity down to 0.000 03 g. Chemical analysis was conducted on those billets using atomic absorption and emission spectrophotometry; the results are shown in Table I. The oxygen content of these billets was determined, before oxidation, using the Leco equipment whereby oxygen is transformed to carbon dioxide and measured by infrared absorption and nitrogen gas by thermal conductivity. The oxygen content of the material is assumed to exist only in SiO_2 and Y_2O_3. Based on this assumption, the compositions of the various billets are located within the ternary system Si_3N_4–SiO_2–Y_2O_3 and are shown in Fig. 1.

The transmission electron microscopy work was performed on a Jeol 100C STEM equipped with a Kevex energy dispersive spectrometer. Thin sections were prepared by cutting Si_3N_4 bars with a low-speed diamond saw to a thickness of 300 μm. These sections were then ground on both 30 and 15 μm metal-bonded diamond discs to a thickness of 90 μm. Discs of 3 mm size were cut from the sections using an ultrasonic disc cutter. The discs were ion milled at 6 keV and 15° tilt using a Gatan ion-beam thinning system until a small hole perforated the sample. The foils were then coated with a thin layer of carbon to prevent charging in the microscope.

A Philips automated powder diffraction system, P1700, was utilized for the X-ray diffraction experiments. The Si_3N_4 samples were ground with tungsten carbide balls in a spex mixer/mill and screened through a 325 mesh sieve prior to X-ray diffraction analysis. Cu$K\alpha$ radiation was used to a generator setting of 40 kV, 40 mA, 0.1° divergence slit and 0.3° receiving slit and the diffracted beam collected by a proportional counter. The samples were scanned at a speed of 0.025 20 sec^{-1} and step interval of 0.02°.

3. Results and observations

Table II and Figs 2 and 3 summarize some of the ambient-temperature flexure strengths (four-point bending); the individual data points on the graph are the average of eight tests. The weight gain is measured after 100 and 200 h exposure at 700° C for the tested Si_3N_4 + Y_2O_3 billets. The Si_3N_4 + 4% Y_2O_3 showed neither anomalous weight gains nor measurable strength reductions. Billet 1959 shows higher strength than that for billets 2755 and 2756 (Fig. 2), owing to its higher Y_2O_3 content (5.54 wt %). The dramatic increase in the flexure strength of billet 1959 after

TABLE I Chemical analysis (wt %) of various Si_3N_4 billets used in the investigation

Billet no. identification	O_2	Y_2O_3	Fe	Al	W	C	N
1761 A	4.6 + 0.003	7.46	0.17	1.8	2.23	2.78	34.8
1959 B	3.6 + 0.06	4.4	0.16	0.14	2.36	2.38	36.7
2755 C	3.2 + 0.01	3.43	0.03	0.05	4.31	1.90	35.7
2756 D	3.4 + 0.09	3.35	0.25	0.21	4.00	2.17	35.3
1546 E	3.9 + 0.06	6.50	0.22	0.17	2.63	2.45	34.7
1974 F	4.2 + 0.03	5.54	–	–	2.36	–	35.2

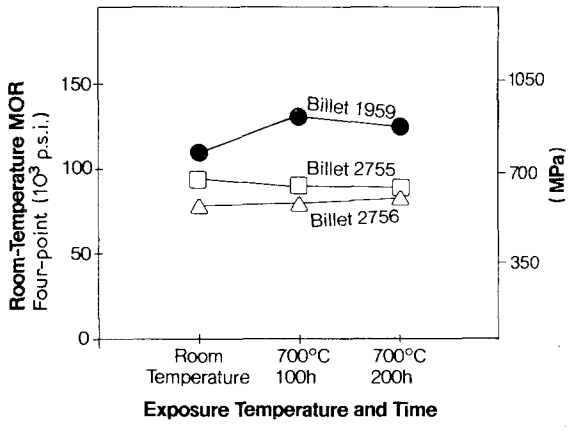

Figure 2 Room-temperature flexture strength for Si_3N_4 billets containing around 4% Y_2O_3, as a function of oxidation temperature and exposure time. Billet 1959 contains 5.54% Y_2O_3; billet 2755 has 3.71% Y_2O_3 and billet 2756 3.35% Y_2O_3.

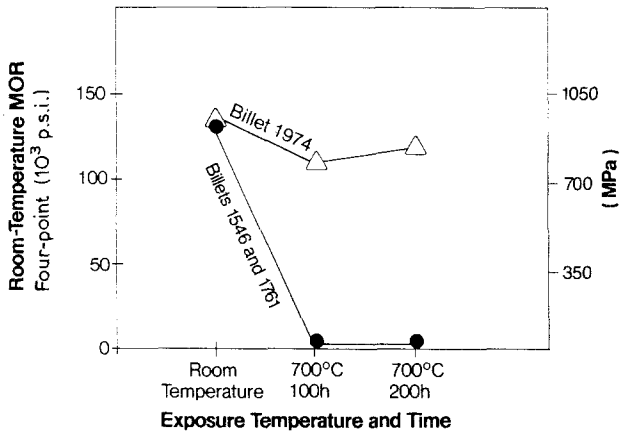

Figure 3 Room-temperature flexture strength for Si_3N_4 containing different amounts of Y_2O_3. Billet 1974 contains 9.41% Y_2O_3, while billet 1546 contains 6.55% Y_2O_3 and billet 1761 has 10.52% Y_2O_3.

TABLE II Room-temperature strengths and weight gains after intermediate temperature oxidation of Si_3N_4 containing different amounts of Y_2O_3

Billet no.	Composition	Starting material	As-received MOR ± S.D.*	700° C exposure			
				100 h		200 h	
				MOR ± S.D.†	Wt gain (%)	MOR ± S.D.†	Wt gain (%)
1959	4% Y_2O_3	N‡ HN-26	111.9 ± 8.3	131.2 ± 5.1	0.012	126.7 ± 7.5	0.008
2756	4% Y_2O_3	N HN-39	78.5§ ± 6.3	78.7 ± 7.5	0.003	83.0 ± 4.5	0.005
2755	4% Y_2O_3	K‖	94.9¶ ± 3.9	90.3 ± 3.0	0.003	87.7 ± 18.0	0.005
1546	8% Y_2O_3	N HN-20	131.1 ± 2.7	**	0.898	**	1.168
1974	8% Y_2O_3	N HN-25	133.4 ± 11.6	111.7 ± 14.9	0.084	118.2 ± 4.2	0.089
1761	8% Y_2O_3	N HN-23	123 ± 3.5	**	1.270	N/A	N/A

*Average of 8 breaks 10^3 p.s.i.
†Average of 4 breaks 10^3 p.s.i.
‡Norton standard HN series Si_3N_4 powder.
§Test bar analysis: 0.21% Al; 0.25% Fe.
‖Kemanord high purity 95P Si_3N_4 powder.
¶Test bar analysis: 0.05% Al; 0.03% Fe.
**Too oxidized and cracked to test.

TABLE III Phase analysis of various Si_3N_4 phases before and after oxidation treatment using X-ray diffraction techniques

	β-Si_3N_4	WSi_2	WC	Si_2ON_2	$Y_2Si_2O_7$	$Y_5N(SiO_4)_3$	SiO_2
Billets with 4% Y_2O_3							
1959 unoxidized	major	minor	trace	–	minor	–	–
1959 700° C 100 h	major	minor	trace	trace	minor	–	–
2755 unoxidized	major	–	minor	minor	trace	–	–
2755 700° C 100 h	major	–	minor	minor	minor	–	–
2756 unoxidized	major	–	minor	minor	trace	–	–
2756 700° C 100 h	major	–	minor	minor	minor	–	–
2756 700° C 100 h discoloured area	major	minor	trace	–	–	minor	–
Billets with 8% Y_2O_3							
1546 unoxidized	major	minor	trace	–	–	minor	–
1546 700° C 100 h catastrophic failure	major	–	trace	–	–	minor	–
1546 700° C 100 h	major	minor	trace	–	–	minor	–
1761 unoxidized	major	minor	trace	–	–	minor	–
1761 700° C 100 h catastrophic failure	major	trace	trace	–	–	minor	–
1974 unoxidized	major	minor	–	–	–	minor	–
1974 700° C 100 h	major	minor	–	–	–	minor	minor

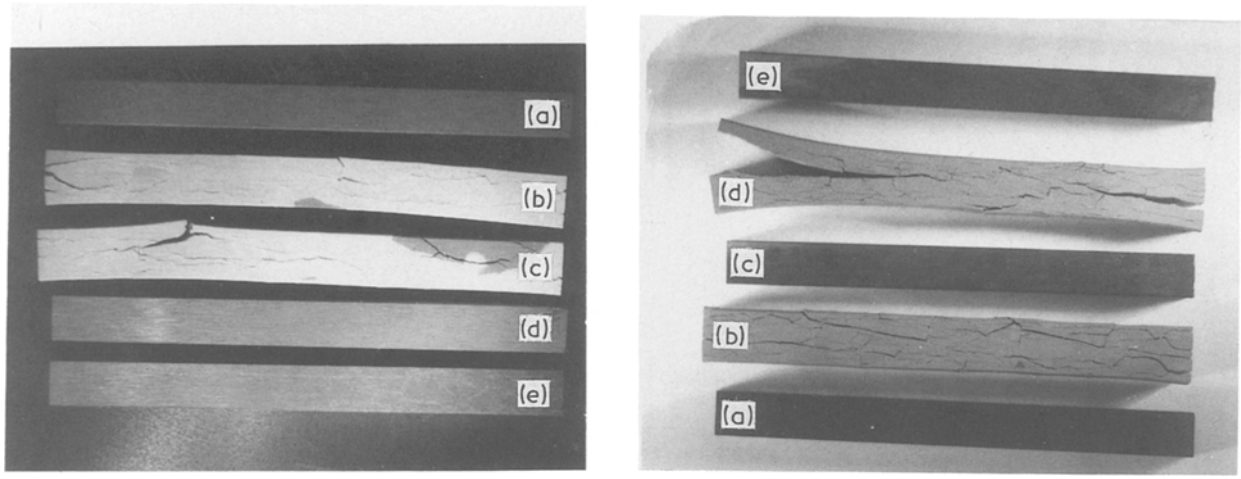

Figure 4 Disintegration of test bars of Si_3N_4 containing 8% Y_2O_3 as a result of oxidation treatment at various temperatures and times. (a) 100 h at a 1000° C, b 800° C, c 700° C, d 500° C, e unexposed. (b) 700° C, a unexposed, b 100 h, c 100 h, d 200 h, e 200 h.

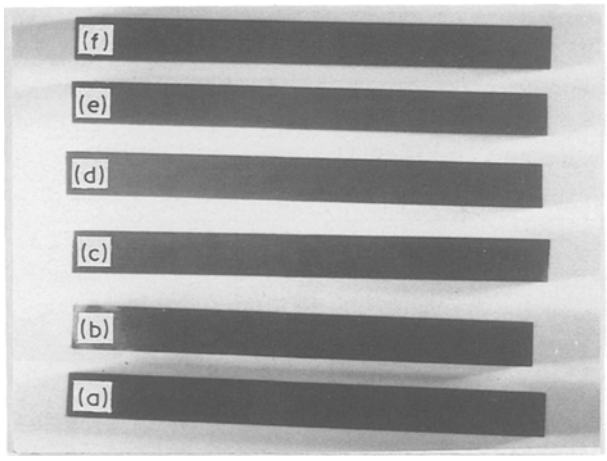

Figure 5 Si_3N_4 + 4% Y_2O_3 test bars showing no disintegration after oxidation in air at 700° C for up to 200 h. a unexposed, b, c, e 100 h, d, f 200 h.

exposure to 700° C oxidation is not within the experimental scatter and may be caused by a stress anneal (healing) of surface-grinding damage of the MOR bars.

All the billets with 8 % Y_2O_3, showed significant weight gains but only two showed severe strength reductions, billets 1761 and 1546. Bars made from those billets disintegrated completely after exposure to both 700 and 800° C in air, see Fig. 4. On the other hand, bars made with 4 % Y_2O_3 did not crack, Fig. 5. After both the 700 and 800° C exposure, some bars of billet 2756 containing 4 % Y_2O_3 showed discoloration (white coating) on the surface – see Fig. 6. Both energy dispersive X-ray microanalysis (EDAX), Fig. 6, and X-ray photoelectron spectroscopy (ESCA) analysis, Fig. 7, reveal that those areas are rich in SiO_2.

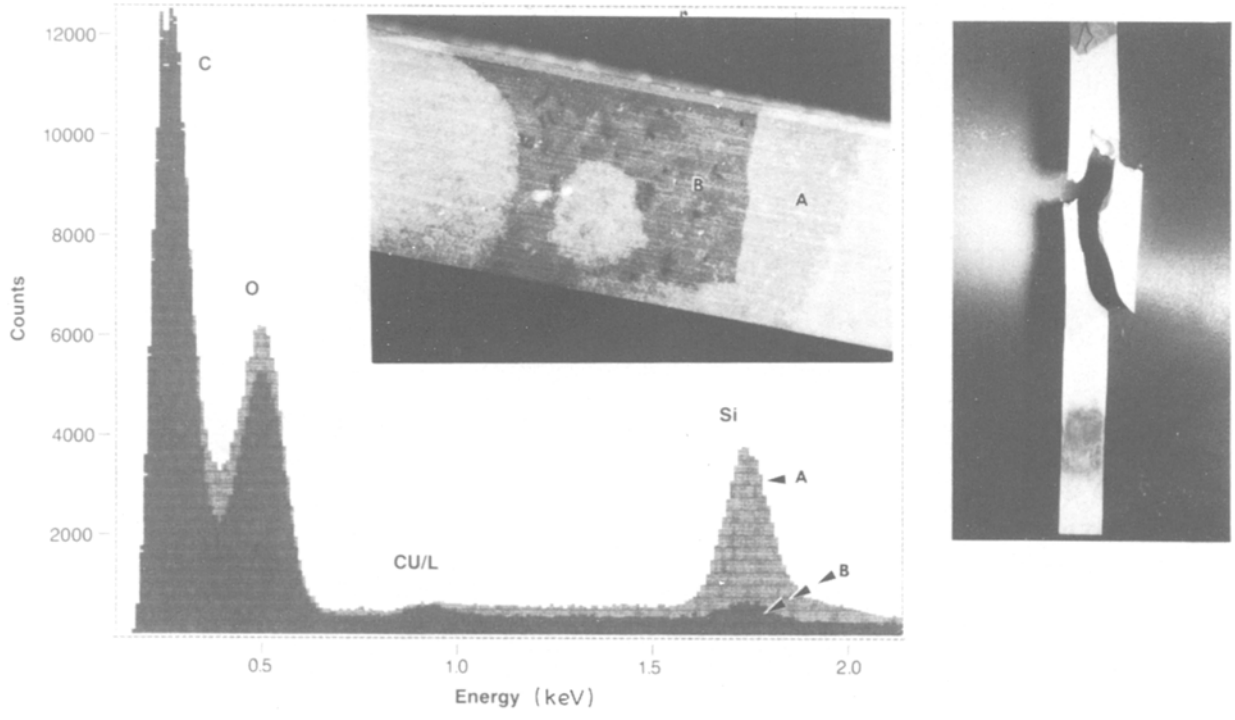

Figure 6 Discoloration of the surface of Si_3N_4 bars as a result of oxidation at 800° C for 100 h. In addition to discoloration, billet 1761 has disintegrated, while billet 2756 did not.

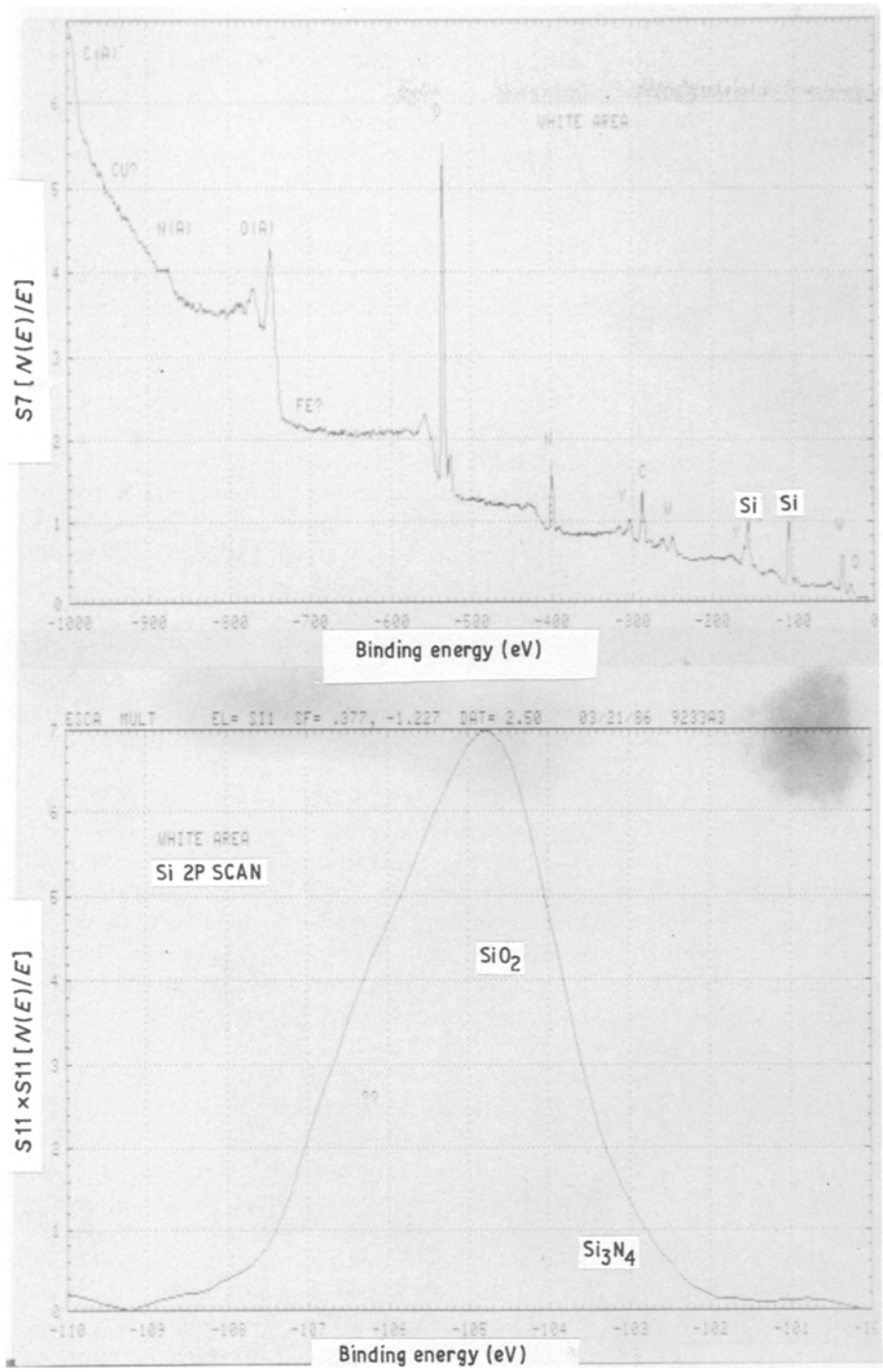

Figure 7 X-ray photoelectron spectroscopy analysis of discoloured regions on the surface of oxidized Si_3N_4.

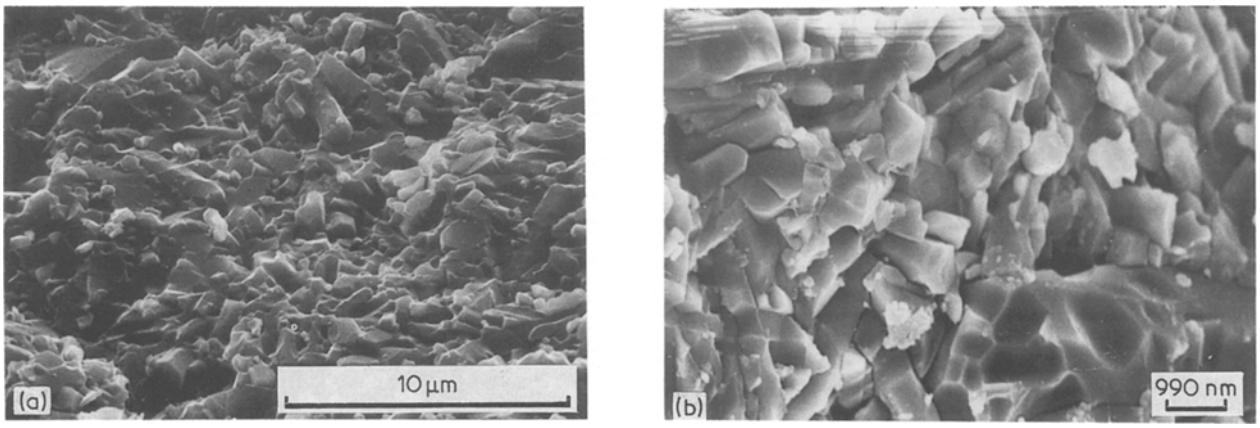

Figure 8 Scanning electron micrographs of the fracture surface of Si_3N_4 containing both (a) 4% Y_2O_3 (billet 1974) and (b) 8% Y_2O_3 (billet 1761) after oxidation treatment. Extensive grain-boundary cracking can be observed in billet 1761.

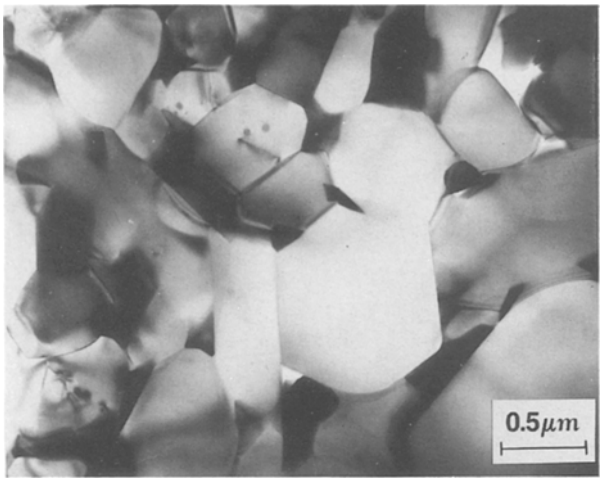

Figure 9 A transmission electron micrograph of Si_3N_4 with 8% Y_2O_3 (billet 1975) showing a broad size distribution of the beta-phase grains.

3.1. Scanning electron microscopy

The fracture surface of the Si_3N_4 + 8% Y_2O_3 material which underwent severe degradation shows extensive grain-boundary cracking, which was absent in those samples which did not degrade, see Fig. 8. The lower yttria content compositions show a mix of intergranular and transgranular failure.

3.2. Transmission electron microscopy

Bright-field images of unoxidized samples show polygonized beta Si_3N_4 grains with a wide size distribution, see Fig. 9, surrounded by a number of grain-boundary phases rich in both tungsten and yttrium. Dark-field images show the presence of a thin glassy film at the β–Si_3N_4 boundaries of all compositions examined, an example is given in Fig. 10. This has also been documented in the literature by other investigators [12]. Samples with 8% Y_2O_3 show the presence of $Y_5N\,(SiO_4)_3$ at the grain boundaries, as confirmed from electron diffraction patterns, see Fig. 11. Extensive substructural changes have also been observed at and near the grain boundaries of Si_3N_4 as a result of oxidation, see Fig. 11, indicating that numerous thermochemical reactions are taking place during the process. The tungsten-containing phases at the β-Si_3N_4 boundaries were identified, from X-ray diffraction, to be WSi_2 and WC, see Fig. 12.

3.3. X-ray diffraction

A summary of the X-ray diffraction study conducted on Si_3N_4 is shown in Table III. Samples with 4% Y_2O_3 show the presence of β-Si_3N_4 as the major phase with minor and trace amounts of other phases including Si_2ON_2, $Y_2Si_2O_7$, WC and WSi_2. These silicon oxynitride phases lie within the compatibility triangle of the ternary Si_3N_4–SiO_2–Y_2O_3 system. No phases outside this triangle have been detected in those samples after they were oxidized. On the other hand, Si_3N_4 compositions containing 8% Y_2O_3 have been detected, in addition to β–Si_3N_4, WC, WSi_2 and $Y_5N\,(SiO_4)_3$ in both the oxidized and non-oxidized state. The presence of $Y_5N\,(SiO_4)_3$, which lies outside the compatibility triangle, has been confirmed by selected-area diffraction, see Fig. 11.

Those compositions containing 8% Y_2O_3, which suffered intermediate temperature oxidation failure show the absence of WSi_2 which existed in the original hot-pressed billets, see Fig. 12. X-ray analysis did not reveal the presence of WO_3 as an oxidation product in those samples.

4. Discussion

The data presented so far clearly indicate that Si_3N_4 material containing 8% Y_2O_3 is thermally unstable in the temperature range 700 to 1000°C, while material with 4% Y_2O_3 does not suffer from the same phenomenon. This instability is apparently related to two major observable differences between these two compositions. The first is the fact that tungsten-containing phases, namely WSi_2 and WC in the 8% Y_2O_3 material which failed catastrophically (billet 1546 as an example), have severely decomposed; most of those tungsten-containing phases existed at the β-Si_3N_4 grain boundaries. Scanning electron microscopy shows that the predominant mode of failure of these compositions is intergranular in nature, see Fig. 8. This may indicate that the process of decomposition of tungsten-containing grain-boundary phases introduce stresses high enough to cause cracking and separation. The second difference

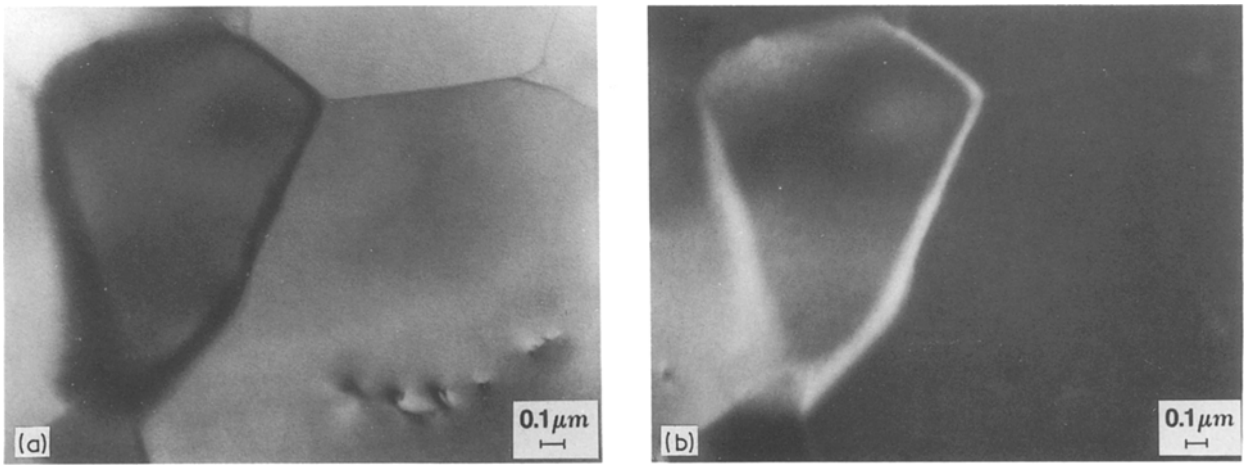

Figure 10 A pair of (a) bright- and (b) dark-field micrographs of billet 1959 which was oxidized in air for 100 h at 1000° C showing the presence of an amorphous phase at the grain boundary of hot-pressed Si_3N_4.

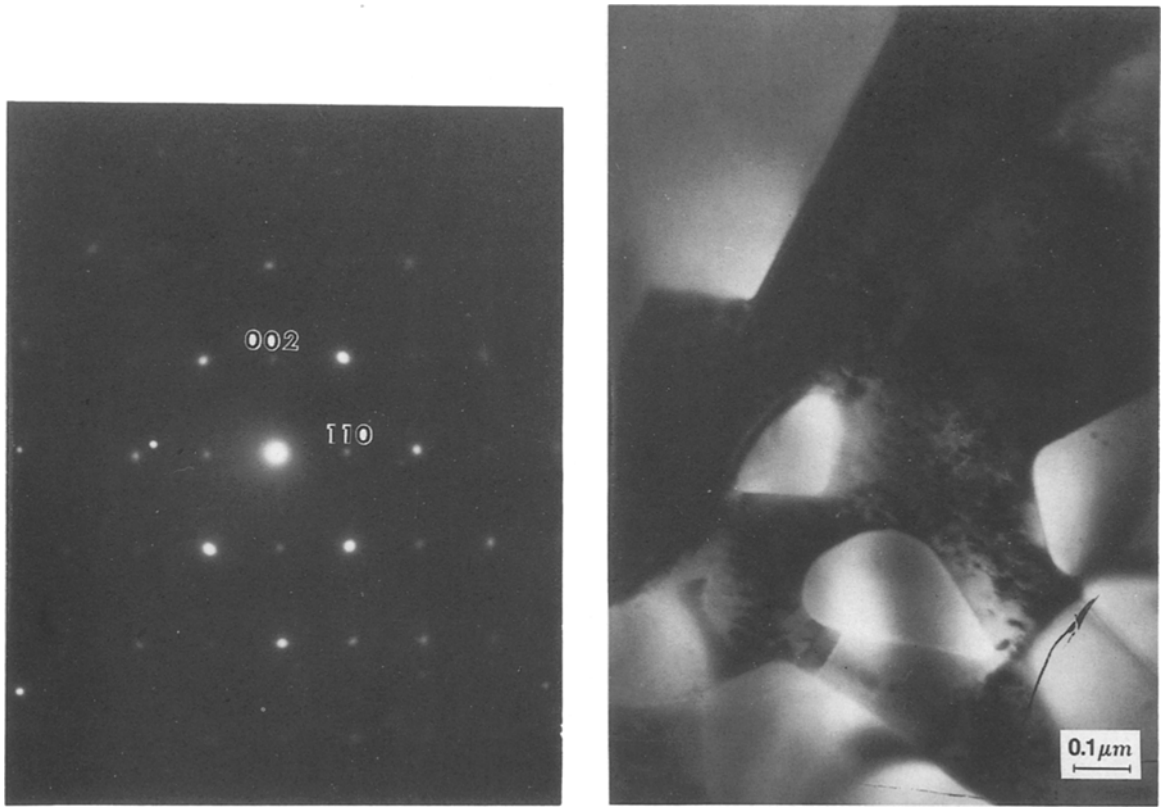

Figure 11 Electron diffraction of Si_3N_4 samples with 8% Y_2O_3 showing the presence of Y_5N $(SiO_4)_3$ phase at the grain boundaries.

between 4% Y_2O_3 material and the 8% Y_2O_3 is the presence of Y_5N $(SiO_4)_3$ phase in those billets with the higher Y_2O_3 content. This phase lies outside the so-called thermally stable region, i.e. Si_3N_4–Si_2ON_2–$Y_2Si_2O_7$ triangle of the ternary system Si_3N_4–SiO_2–Y_2O_3. Although no experiment has yet been designed to measure the volume change/residual stresses introduced during formation and/or decomposition of those undesirable phases (outside the compatibility region), Lange and others postulated that this is the main reason for the material's catastrophic failure at intermediate temperatures. The fact that significant substructural changes have been observed at and near the 8% Y_2O_3 material's grain boundaries as a result of oxidation indicate that Lange's explanation is not sufficient, because some of these undesirable phases

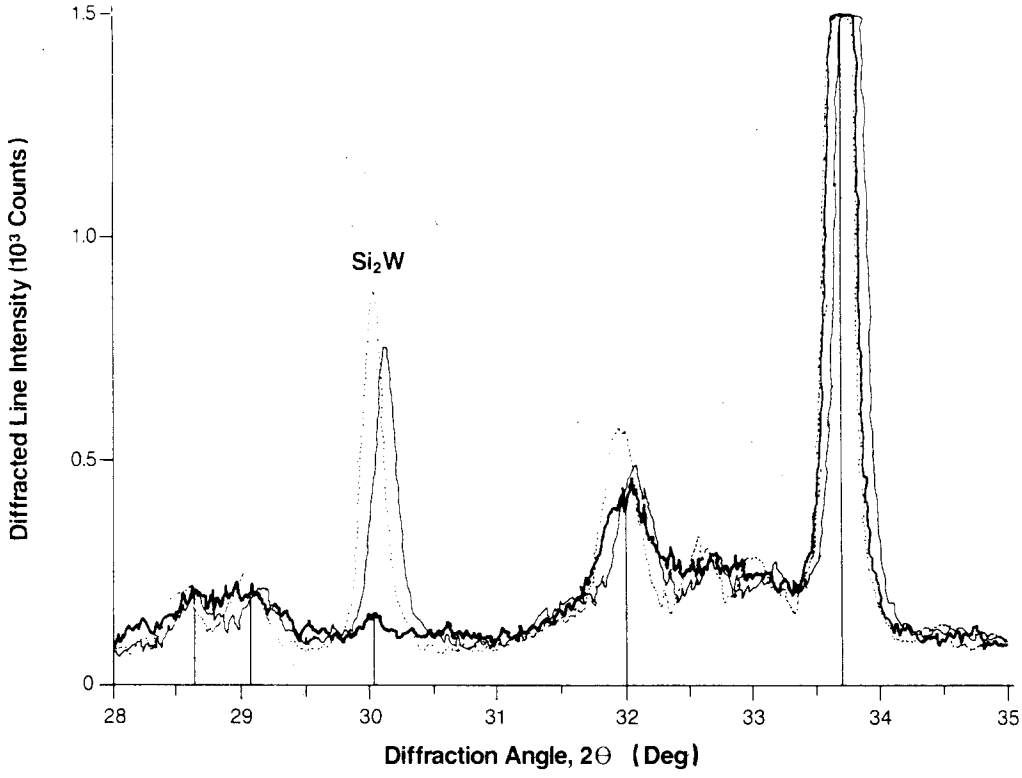

Figure 12 X-ray diffraction pattern of billet 1546 (8% Y_2O_3) showing the effect of oxidation on the stability of WSi_2. (. . .) 1546 unoxidized; (——) 1546, 700° C, 100 h; (——) 1546, 700° C, 100 h; catastrophic failure.

existed in some billets that did not fail. More work is needed to reveal intricate substructural changes at the material's grain boundaries after oxidation using compositional line profile and diffusion studies to help quantify those microstructural changes in relationship to the oxidation process.

5. Conclusions

1. Si_3N_4 compositions containing 4% Y_2O_3 did not undergo the degradation effects observed in the 8% Y_2O_3 material during oxidation at 500 to 1000°C.

2. The material with the 4% Y_2O_3 contains the phases Si_2ON_2, $Y_2Si_2O_7$, and β-Si_3N_4 which are within the compatibility triangle. On the other hand, the material with 8% Y_2O_3 contains $Y_5N(SiO_4)_3$ which is outside the triangle.

3. The oxidation process resulted in decomposition and disappearance of WSi_2 from the grain boundaries of Si_3N_4 with 8% Y_2O_3 which underwent severe cracking.

4. Transmission electron microscopy work reveals the presence of substructural features at and near the boundaries of oxidized β-Si_3N_4 grains; those features did not exist in the non-oxidized material.

Acknowledgements

The authors acknowledge the help of Mr D. J. Devlin with the X-ray diffraction experiments. Review of the manuscript by Dr J. N. Panzarino is appreciated.

References

1. U. R. EVANS, "The Corrosion and Oxidation of Metals" (Edward Arnold, London, 1960).
2. S. C. SINGHAL, *J. Mater Sci* **11** (1976) 500.
3. F. F. LANGE, S. C. SINGHAL and R. C. KUZNICKI, *J. Amer. Ceram. Soc.* **60** (1977) 249.
4. G. E. GAZZA, "Influence of Composition and Process Selection on Densification of silicon Nitride", AMMRC TR-82-32, AD/A116-652-US Department of Commerce, NTIS (1982).
5. J. A. MANGELS and J. R. BAR, US Pat. 4388414 (1983).
6. A. ARIAS, "Effect of Yttria Additions on Properties of Pressureless Sintered Silicon Nitride", NASA Technical Paper 1899 (1981).
7. G. Q. WEAVER and J. W. LUCEK, *Amer. Ceram. Soc.* **57** (1978) 1131.
8. J. W. LUCEK, "Silicon Nitride – Yttrium Oxide – Thermal Instability", Norton internal report (1984).
9. R. R. GOVILA, J. A. MANGELS and J. R. BAER, *Amer. Ceram. Soc.* **68** (1985) 413.
10. C. L. QUACKENBUSH, "GTE Si_3N_4 – Based Ceramics", Highway Vehicles Systems Contracts Coordination Meeting – 24–26 April 1979, Dearborn, Michigan.
11. S. SCHOUN, "Effect of W and WC on the Oxidation Resistance of Yttria Doped Si_3N_4", NASA Report 81529 (1982).
12. S. DUTTA, *Amer. Ceram. Soc. Commun. C-2* **65** No. 1 (1982).

Received 16 September 1988
and accepted 24 February 1989